



## Get Clarity On Generics

Cost-Effective CT & MRI Contrast Agents

 FRESENIUS  
KABI

[WATCH VIDEO](#)

# AJNR

This information is current as  
of August 11, 2025.

## **Brain Nuclear Magnetic Resonance Imaging Enhanced by a Paramagnetic Nitroxide Contrast Agent: Preliminary Report**

Robert C. Brasch, Danute E. Nitecki, Michael Brant-Zawadzki,  
Dieter R. Enzmann, George E. Wesbey, Thomas N. Tozer, L.  
Dallas Tuck, Christopher E. Cann, John R. Fike and Phillip  
Sheldon

*AJNR Am J Neuroradiol* 1983, 4 (5) 1035-1039  
<http://www.ajnr.org/content/4/5/1035>

# Brain Nuclear Magnetic Resonance Imaging Enhanced by a Paramagnetic Nitroxide Contrast Agent: Preliminary Report

Robert C. Brasch<sup>1</sup>  
 Danute E. Nitecki<sup>1</sup>  
 Michael Brant-Zawadzki<sup>1</sup>  
 Dieter R. Enzmann<sup>2</sup>  
 George E. Wesbey<sup>1</sup>  
 Thomas N. Tozer<sup>3</sup>  
 L. Dallas Tuck<sup>3</sup>  
 Christopher E. Cann<sup>1</sup>  
 John R. Fike<sup>4</sup>  
 Phillip Sheldon<sup>1</sup>

Contrast-enhancing agents for demonstrating abnormalities of the blood-brain barrier may extend the diagnostic utility of proton nuclear magnetic resonance (NMR) imaging. "TES," a nitroxide stable free radical derivative, was tested as a central nervous system contrast enhancer in dogs with experimentally induced unilateral cerebritis or radiation cerebral damage. After intravenous injection of TES, the normal brain showed no change in NMR appearance, but areas of disease demonstrated a dramatic increase (up to 45%) in spin-echo intensity and a decrease in T<sub>1</sub> relaxation times. The areas of disease defined by TES enhancement were either not evident on the nonenhanced NMR images or were better defined after contrast administration. In-depth tests of toxicity, stability, and metabolism of this promising NMR contrast agent are now in progress.

Contrast-enhancing pharmaceutical agents may extend the diagnostic capabilities of nuclear magnetic resonance (NMR) imaging. Paramagnetic substances tested as NMR contrast agents include the ions of manganese and iron and nitroxide stable free radicals (NSFRs) [1, 2]; all have been shown to decrease proton relaxation times, namely T<sub>1</sub> and T<sub>2</sub> [3]. Thus, paramagnetic substances enhance contrast differences between those tissues containing the contrast agent and magnetically similar tissues without it.

In separate reports we have described the relative advantages and disadvantages of various methods to manipulate NMR contrast [2, 4] and the potential to directly evaluate renal function in experimental animals using NSFRs as urographic NMR contrast agents [2, 5].

NSFRs are a group of synthetic, strongly paramagnetic organic compounds that for two decades have been used as "spin labels" for in vitro biologic studies [6]. A water-soluble piperidinyI NSFR derivative, "TES," is rapidly excreted into the urine after intravenous administration, an excretion pattern useful for NMR urographic studies [2, 5]. TES demonstrates additional properties suggesting promise as a clinically useful NMR contrast agent; these include chemical stability of solutions over a broad range of pH and temperature, limited in vivo metabolism, and broad chemical versatility [2, 6]. The ability to chemically attach TES to a variety of biomolecules, drugs, and particles may permit the synthesis of tissue-specific NMR contrast agents. Preliminary toxicity studies of NSFRs, the subject of future reports, are also favorable for the continued development of NSFRs as pharmaceuticals.

In this study we examined the potential of TES to enhance NMR contrast within the brains of animals having experimentally induced cerebritis or radiation damage. Living dogs were imaged by NMR before and after intravenous administration of TES. Loci of brain injury were more clearly identified on the postcontrast images; TES appears to cross the blood-brain barrier (BBB) only at sites of disease and thereby increases the diagnostic yield from the NMR imaging examination.

This article appears in the September/October 1983 issue of *AJNR* and the November 1983 issue of *AJR*.

Received October 29, 1982; accepted after revision February 14, 1983.

Presented at the Symposium Neuroradiologicum, Washington, DC, October 1982.

This work was supported in parts by grants from the Dean of Medicine, University of California, San Francisco; Radiology Research and Education Foundation, University of California, San Francisco; and National Institutes of Health grants R01 AM 31937, National Institute of Arthritis, Diabetes, Digestive and Kidney Diseases, and CA-30445, National Cancer Institute.

<sup>1</sup> Department of Radiology, University of California School of Medicine, San Francisco, CA 94143. Address reprint requests to R. C. Brasch.

<sup>2</sup> Department of Radiology, Stanford University School of Medicine, Stanford, CA 94305.

<sup>3</sup> Department of Pharmaceutical Chemistry, University of California School of Medicine, San Francisco, CA 94143.

<sup>4</sup> Department of Radiation Therapy, University of California School of Medicine, San Francisco, CA 94143.

*AJNR* 4:1035-1039, September/October 1983  
 0195-6108/83/0405-1035 \$00.00  
 © American Roentgen Ray Society



## Materials and Methods

### Experimental Animals

Alpha-streptococcus brain abscesses were produced in two mongrel dogs using a procedure described previously [7]. Briefly, a bacteria agarose mixture ( $10^8$ – $10^9$  alpha streptococci) was injected through a burr hole to a depth of 3–4 mm into the left parietal cortex. The infected dogs, weighing 15 and 25 kg, were imaged on postoperative day 6 (late cerebritis stage) or postoperative day 13 (early capsule stage) by computed tomographic (CT) (Varian) and NMR techniques. CT brain scans were obtained before and 30 min after intravenous administration of methylglucamine iohalamate 60% (1 ml/kg).

In a third mongrel dog, 16 kg, cerebral radiation damage was induced using a removable  $^{125}\text{I}$  source (3M Co.) placed through a burr hole into the right parietal white matter adjacent to the lateral ventricle for a period of 3 days. The source strength was 31.9 mCi (1,180.3 MBq). The radiation dose was 3,000 rad (30 Gy) 1 cm from the source. CT imaging was performed at monthly intervals using a General Electric 7800 scanner with and without iohalamate contrast enhancement. Four months after brain irradiation the animal was imaged using NMR.

All three dogs were sacrificed following the NMR imaging procedure and brain tissue samples were obtained for *in vitro* nitroxide measurement by electron spin resonance spectrometry and for histologic evaluation. The histologic specimens were fixed in 10% formalin for a period of at least 5 weeks before routine hematoxylin and eosin staining.

CT and NMR images were qualitatively compared for diagnostic content and particularly for contrast enhancement. *In vitro* measurements of nitroxide tissue concentrations and histologic data were used to verify the imaging data.

### NMR Imaging

Our NMR imaging unit, previously described in detail [8], uses a 3.5 kG superconducting magnet. High-resolution mode yielded pixels of  $1.6 \times 1.4$  mm (XY) on a  $128 \times 128$  matrix. Five contiguous 7 mm transverse sections through the brain were sampled in a 13 min period. Four separate spin-echo intensity images were obtained for each section, each based on a different instrument setting for pulse interval "a" (0.5 or 1.0 sec) or echo sampling "b" (28 or 56 msec). The spin-echo sequence utilizes a  $90^\circ$  radiofrequency pulse followed by two  $180^\circ$  pulses. From these intensity data, estimated  $T_1$  and  $T_2$  relaxation values, given in milliseconds, were calculated. A computer program permitted averaging of intensity (I),  $T_1$ , and  $T_2$  relaxation values for selected regions of interest. Such region-of-interest measurements were made for multiple areas of the brain before and after administration of NMR contrast agent.

### Preparation of NSFR Contrast Agent

The general structure of a piperidiny NSFR compound "TES" is shown in figure 1. An unpaired electron within this NSFR compound confers paramagnetic properties. This electron is protected from chemical interaction by steric hindrance provided by four methyl groups on the alpha carbons and by delocalization of the unpaired electron toward the center of the molecule. TES, synthesized in our laboratory, was stored as dry powder or as a concentrated aqueous solution, buffered to pH 7.2, before intravenous administration. The dose of TES, chosen arbitrarily, was 0.9 g/kg body weight.

### Nitroxide Concentration in Tissue Samples

Samples of brain tissue (30–250 mg) were homogenized in 2N sodium hydroxide and kept for 24 hr at room temperature to extract

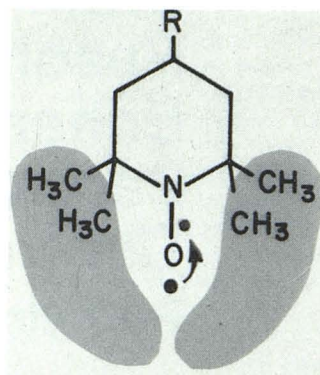


Fig. 1.—Stability of nitroxide stable free radicals (NSFRs) can be attributed in part to steric hindrance provided by bulky methyl groups on alpha carbons (shaded area) and in part to delocalization of unpaired electron (dot with arrow) from nitrogen toward oxygen atom. Piperidine derivative shown here is just one of several classes of NSFRs. Various substitutions at position R make it possible to meet specific requirements of different biologic systems and may permit selective tissue targeting of NSFR contrast molecule. (Reprinted from [5].)

TES. After filtration, the extracts were measured for nitroxide concentration by electron spin resonance spectrometry. Freshly prepared nitroxide solutions of known concentrations were used as standards.

Our electron spin resonance spectrometer, previously described [9] and modified with a Varian 100 kcycle field modulation and control unit and a multipurpose cavity, was used to measure nitroxide concentrations within extracts of autopsied nervous tissue. The aqueous extracts were placed in a Varian flat cell with a volume of 0.04 ml within the microwave cavity.

## Results

Experimentally induced cerebritis was demonstrated on both CT and NMR images. The CT manifestations of cerebritis in our study confirmed those previously reported [7] and included peripheral contrast enhancement with gradual diffusion of contrast material into the central, low-density part of the lesion. The peripheral area of contrast enhancement on the CT images correlated best with the extensive surrounding cerebritis. The central, low-density area seen on the CT corresponded to the pathologically demonstrated necrotic center. The CT scan in both the late cerebritis and the early capsule stages retained this pattern of peripheral enhancement. The extent of surrounding inflammation tended to regress by the early capsule stage (day 13), and the area of contrast enhancement became more circumscribed corresponding to the development capsule (figs. 2A and 2B).

The brain infections, well seen on the nonenhanced NMR images, were depicted as high-intensity rings with low-intensity central necrotic areas. The nonenhanced NMR appearance of these brain abscesses has recently been fully described [10].

An obvious contrast-enhancing effect was noted on the NMR images after intravenous administration of TES. In the late cerebritis stage (day 6) the size of the abnormality on TES-enhanced images was considerably larger than on the nonenhanced images (fig. 3). TES produced a marked increase of intensity within the central part of the lesion attributed to diffusion of contrast molecules into the necrotic core. The apparent increase in overall area of the lesion after contrast enhancement is probably due to diffusion of contrast material into the surrounding regions of brain edema.



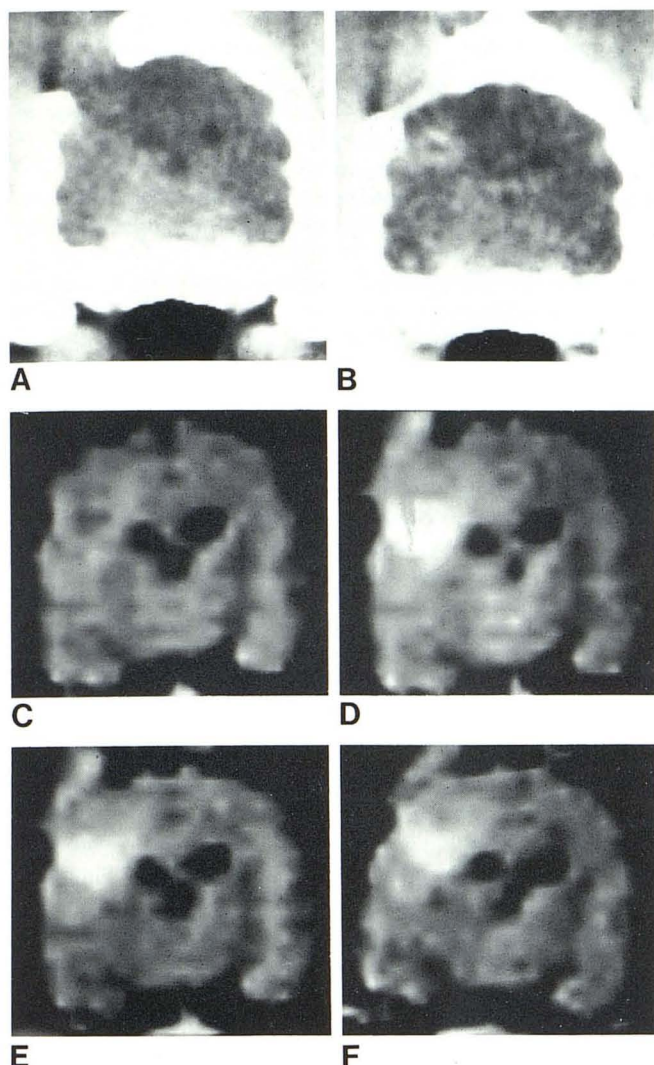


Fig. 2.—Dog with abscess in early capsule stage. Coronal CT scans before (A) and after (B) intravenous administration of iohalamate (1 ml/kg). (This animal moved slightly between pre- and postcontrast scans.) Circumscribed pattern of contrast enhancement corresponded to developing capsule. NMR spin-echo images ( $a = 28$  msec;  $b = 1.0$  sec) through same anatomic section before (C) and 10 (D), 20 (E), and 60 (F) min after intravenous administration of TES. C, Low-intensity central focus is surrounded by rim of higher intensity, which pathologically corresponds to developing capsule. Contrast enhancement of lesion is maximum in E and is partly faded by F. D–F showed marked increase in intensity at periphery of lesion and within central necrotic core. Incidental finding is contrast enhancement in soft tissues overlying site of prior craniotomy, possibly reflecting local vascular damage.

There also appeared to be a “blush” on the walls of the lateral ventricles after contrast enhancement. Similar observations have been noted with contrast-enhanced CT images [11]. The explanation for this phenomenon is unknown but may be related to the subependymal veins [12].

In the early capsule stage (day 13) there was also a marked increase in intensity within the abscess (10, 20, and 60 min) after TES administration (figs. 2C–2F). In the center of the abscess the intensity (mean  $\pm$  SD) increased 45% ( $2.2 \pm 0.08$  to  $3.2 \pm 0.14$ ) by 20 min. The periphery of the abscess was also enhanced in a discrete circular pattern,

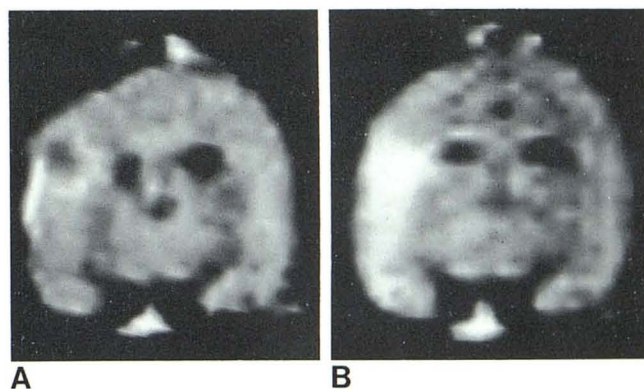


Fig. 3.—Dog with late cerebritis. NMR spin-echo images ( $a = 28$  msec;  $b = 1.0$  sec) before (A) and 20 min after (B) TES administration show contrast-enhancing effect in cerebral cortex at abscess site. Contrast agent produces increase in intensity in central, necrotic core of cerebritis lesion as well as diffuse peripheral contrast enhancement around inflammatory lesion. Overall size of lesion appears larger after contrast administration. Also noted is increase in intensity or “blush” in ventricular walls.

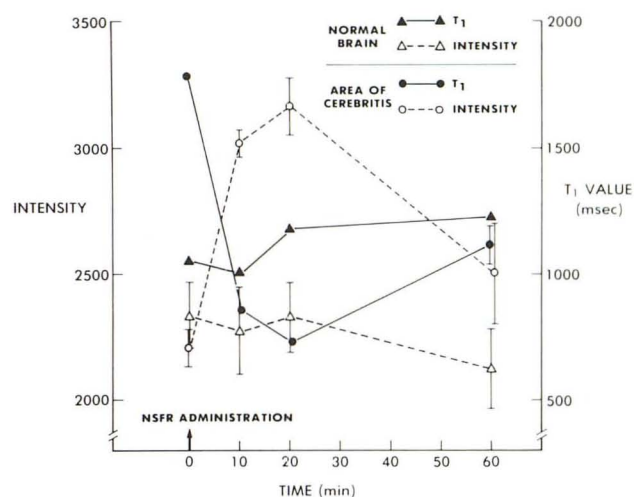


Fig. 4.—Same dog as in fig. 2, with early capsule inflammatory lesion. Area-of-interest measurements from normal right cerebral white matter and left-sided area of cerebritis show significant increase in intensity and simultaneous decline in  $T_1$  relaxation times in area of cerebritis. Contrast-enhancing effect is maximum at 20 min.

not diffusely as in the late cerebritis lesion. The degree of contrast enhancement diminished by 60 min when the animal was sacrificed. Correspondingly,  $T_1$  values decreased in the center and rim of the abscess after TES administration (fig. 4).  $T_2$  values remained relatively constant on the pre- and postcontrast calculations (70 and 62 msec, respectively).  $T_2$  values of the normal brain varied from 66 to 59 msec.

The electron spin resonance measurements of tissue nitroxide concentration showed a large difference in concentration 1 hr postinjection between the abscess and the contralateral unaffected brain. The necrotic center of the abscess had a concentration of 0.45 mM/g and the rim of the abscess had a concentration of 0.66 mM/g. At a dis-



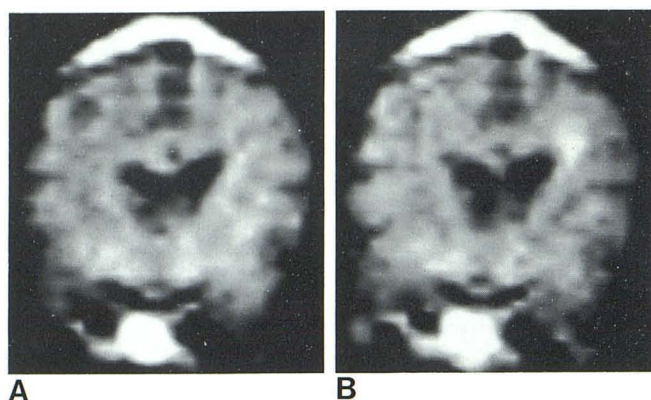


Fig. 5.—Dog with radiation-induced damage in right, periventricular white matter. NMR spin-echo images ( $a = 28$  msec;  $b = 1.0$  sec). **A**, Precontrast image shows ventricular asymmetry but no focal intensity abnormality in damaged region. **B**, 30 min after contrast. Focus of increased intensity at site of pathologically confirmed noninflammatory necrosis.

tance of 1 cm from the rim there was a detectable accumulation of nitroxide, 0.1 mM/g. Four tissue samples taken from the contralateral (right) cerebral cortex had no detectable nitroxide activity by electron spin resonance, indicating less than 0.03 mM/g.

For the animal with experimentally induced radiation damage NMR demonstrated ventricular asymmetry on the non-enhanced images but no focal abnormality could be detected (intensity,  $T_1$  or  $T_2$  images). NMR images obtained after TES administration showed an obvious area of increased intensity in the right cerebrum adjacent to the lateral ventricle, the site of  $^{125}\text{I}$  source implantation 4 months before (fig. 5). The lesion intensity (mean value  $\pm$  SD) was slightly higher on the 30 min image than on the 10 min image. The lesion intensity increased from  $1.6 \pm 0.11$  (precontrast) to  $1.9 \pm 0.19$  (30 min postcontrast) in the region of radiation damage. The corresponding contralateral cerebral tissue maintained a uniform intensity ( $1.7 \pm 0.11$  precontrast and postcontrast). The observed change in intensity within the damaged brain was again associated with a decrease in  $T_1$  relaxation values from 1,045 precontrast to 624 30 min after TES administration.  $T_2$  values did not change significantly (54 to 56 msec).

Pathologically  $^{125}\text{I}$  irradiation produced white-matter atrophy, noninflammatory coagulation necrosis, and edema. Fibrinoid necrosis of vessel walls with adjacent spongiosis and gliosis were observed [13].

Electron spin resonance analysis of pathologic and normal brain specimens showed no detectable nitroxide within the normal left cerebrum (less than 0.008 mM/g). In the region of radiation necrosis, a nitroxide concentration of 0.02 mM/g was observed.

## Discussion

The mechanism of TES contrast enhancement is attributable to its strong paramagnetic properties. Paramagnetic substances when placed in a magnetic field exert a relaxing

effect on hydrogen nuclei in the microchemical environment. This effect, termed "proton relaxation enhancement," produces a decrease in  $T_1$  and  $T_2$  relaxation values of neighboring hydrogen nuclei [3]. Our data indicate that the decrease in  $T_1$  values is relatively greater than the change in  $T_2$  values at the concentrations of TES employed. The proton relaxation enhancement effects are temporary and disappear when the paramagnetic contrast agent is cleared from the tissue.

Numerous reports demonstrate the utility of NMR imaging for the identification and diagnosis of central nervous system disease [14–16]. For certain conditions including demyelinating disease and brainstem infarction, NMR appears to be more useful than CT. To date, one of the possible disadvantages of NMR has been the lack of contrast agents to identify subtle breaks in the BBB [14].

NSFRs potentially fulfill this role and, if developed into clinically employed pharmaceuticals, may extend the diagnostic sensitivity and specificity of the NMR technique. Although our experiments include only two types of cerebral pathology (bacterial cerebritis and radiation necrosis), the results vividly demonstrate a contrast-enhancing effect of TES in abnormal tissues when compared with normal, non-enhanced tissues. The pathophysiology of NSFR accumulation in abnormal tissues is postulated to be the same as that of the commonly used radiographic agents; in particular, contrast molecules leak into the brain substance only in regions of BBB breakdown. Contrast enhancement of BBB defects by CT imaging is widely used and clinically valuable; the clinical role of parallel contrast agents for NMR imaging remains to be determined.

The time course of TES accumulation and clearance from brain lesions appears to be well suited to clinical use. After intravenous injection, the contrast effects (decreased  $T_1$  values and increased intensity) were maximum in the brain lesions from 20 to 30 min after administration and tended to diminish by 1 hr. The renal clearance of TES in the healthy cat is 10 ml/min, a value approximating glomerular filtration. Half-life of TES in the cat is about 38 min [2, 5]. Thus, the entire bolus of vascular contrast agents should be eliminated from the body within a few hours. More detailed studies of NSFR distribution, clearance, and metabolism are in progress.

Our studies are inadequate to indicate an "ideal" or a "least-possible-but-useful" dose for TES in demonstrating cerebral lesions. From previous *in vitro* studies we have shown a 40% intensity increase of aqueous solutions of 1.0 mM TES [2]. By narrowing the NMR gray scale, as is the routine practice in CT scanning, it may be possible to readily identify intensity alterations of 5% or less. Thus, the levels of contrast enhancement achieved in our animal, as high as 45% intensity increase above background, exceed the necessary or even the desired contrast enhancement. The TES dose of 0.9 g/kg of body weight was chosen arbitrarily and can surely be reduced in future studies without loss of contrast effect. The appropriate dose of the NMR contrast agent may also decrease in future studies as the resolving capabilities of NMR improve, a likely prediction based on recent trends.

## REFERENCES

1. Goldman MR, Brady TJ, Pykett IL, et al. Application of NMR imaging to the heart. *Radiology* **1982**;142:246-248
2. Brasch RC, Nitecki DE, London D, et al. Evaluation of nitroxide stable free radicals for contrast enhancement in NMR imaging (abstr). *J Nuclear Magnetic Resonance Med.* (in press)
3. Slichter CP. *Principles of magnetic resonance*. New York: Harper & Row, **1963**:1-50, 137-183
4. Brasch RC. Methods of contrast enhancement for NMR imaging and potential applications. *Radiology* **1983**;147:781-788
5. Brasch RC, Tozer TN, London DA, et al. Nuclear magnetic resonance study of a paramagnetic nitroxide contrast agent for enhancement of renal structures in experimental animals. *Radiology* **1983**;147:773-779
6. Stone TJ, Buckman T, Nardio PL, McConnell HM. Spin-labeled biomolecules. *Proc Natl Acad Sci USA* **1965**;54:1010-1017
7. Enzmann DR, Britt RH, Yeager AS. Experimental brain abscess evaluation; computed tomographic and neuropathologic correlation. *Radiology* **1979**;133:113-122
8. Crooks L, Arakawa M, Hoenninger J, et al. Nuclear magnetic resonance whole-body imager operating at 3.5 KGauss. *Radiology* **1982**;143:169-174
9. Tuck LD, Schieser DW. Electron spin resonance of some nitrogen-containing aromatic free radicals. *J Phys Chem* **1962**;66:937-939
10. Brant-Zawadzki M, Enzmann DR, Placone RC Jr, et al. NMR imaging of experimental brain abscess: comparison with CT. *AJNR* **1983**;4:250-253
11. Naidich TP, Padlowski RM, Leeds NE, Naidich JB, Chisholm AJ, Rifkin MD. The normal contrast-enhanced computed axial tomogram of the brain. *J Comput Assist Tomogr* **1977**;1:16-29
12. Sage MR. Blood-brain barrier: phenomenon of increasing importance to the imaging clinician. *AJNR* **1982**;3:127-138, *AJR* **1982**;138:887-898
13. Fike JR, Cann CE, Berstein M, et al. Radiation damage to the canine brain after  $^{125}\text{I}$  implantation (abstr). *Radiat Res* **1982**;91:370
14. Bydder GM, Steiner RF, Young IR, et al. Clinical NMR imaging of the brain: 140 cases. *AJNR* **1982**;3:459-480, *AJR* **1982**;139:215-236
15. Young IR, Hall AS, Pallis CA, Legg NJ, Bydder BM, Steiner RE. Nuclear magnetic resonance imaging of the brain in multiple sclerosis. *Lancet* **1982**;2:1063-1066
16. Brant-Zawadzki M, Davis PL, Crooks LE, et al. NMR demonstration of cerebral abnormalities: comparison with CT. *AJNR* **1983**;4:117-124, *AJR* **1983**;140:847-854